graphene

the mother of all carbon nanostructures

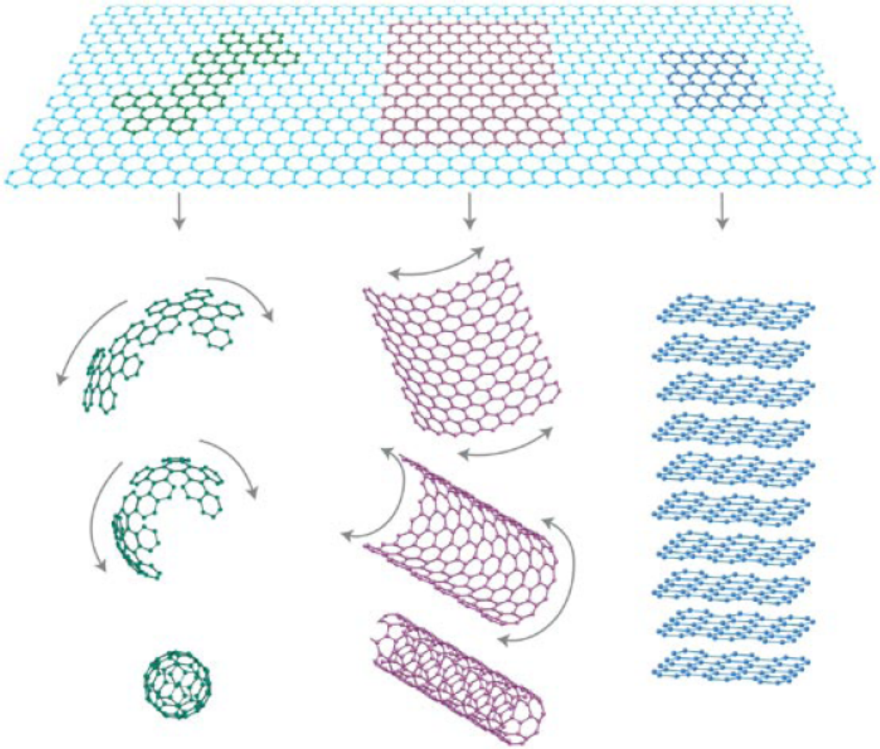

CNTs discover

A paper by Oberlin, Endo, and Koyama published in 1976 clearly showed hollow carbon fibers with nanometer-scale diameters using a vapor-growth technique (Oberlin, A.; M. Endo, and T. Koyama, J. Cryst. Growth (March 1976). *Filamentous growth of carbon through benzene decomposition*. **32**. pp. 335–349.)

Iijima, Sumio (1991). "Helical microtubules of graphitic carbon". *Nature* **354**: 56–58.

Fullerenes

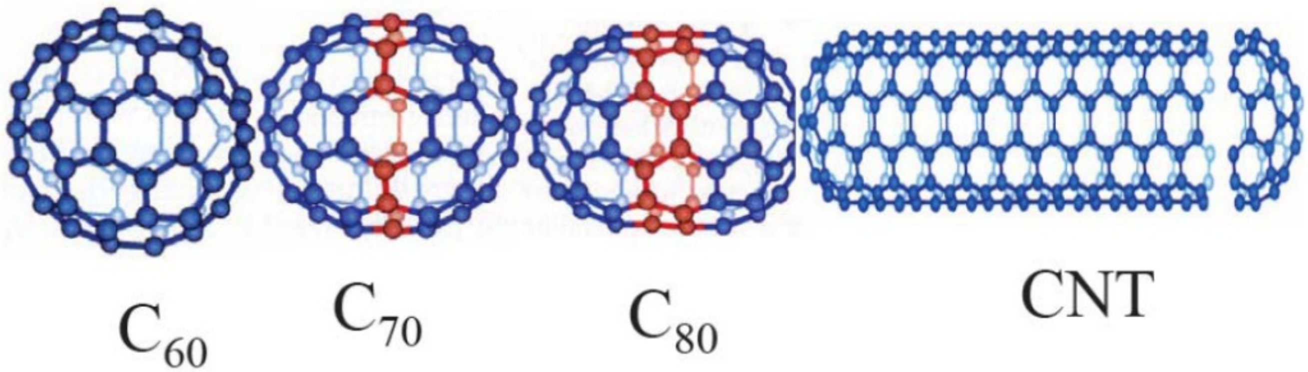

nanotubes

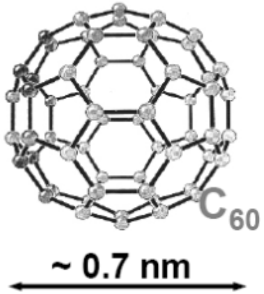

Fullerenes

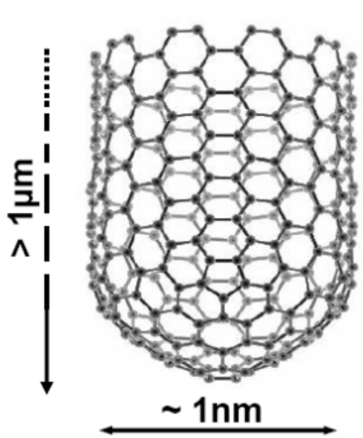

Nanotubes

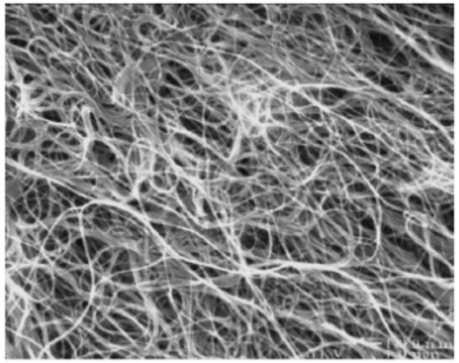

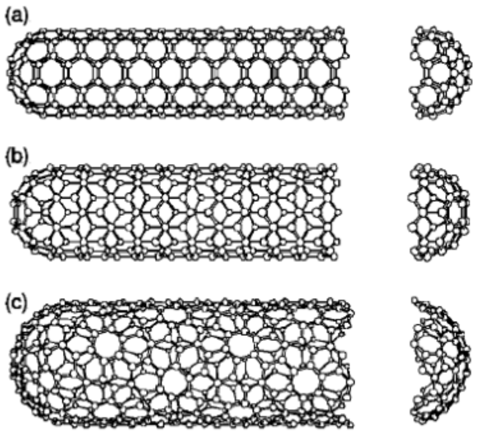

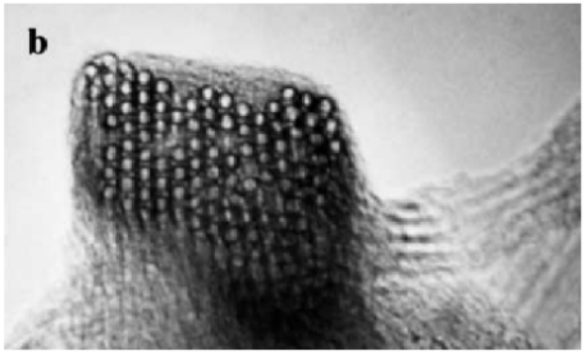

structure

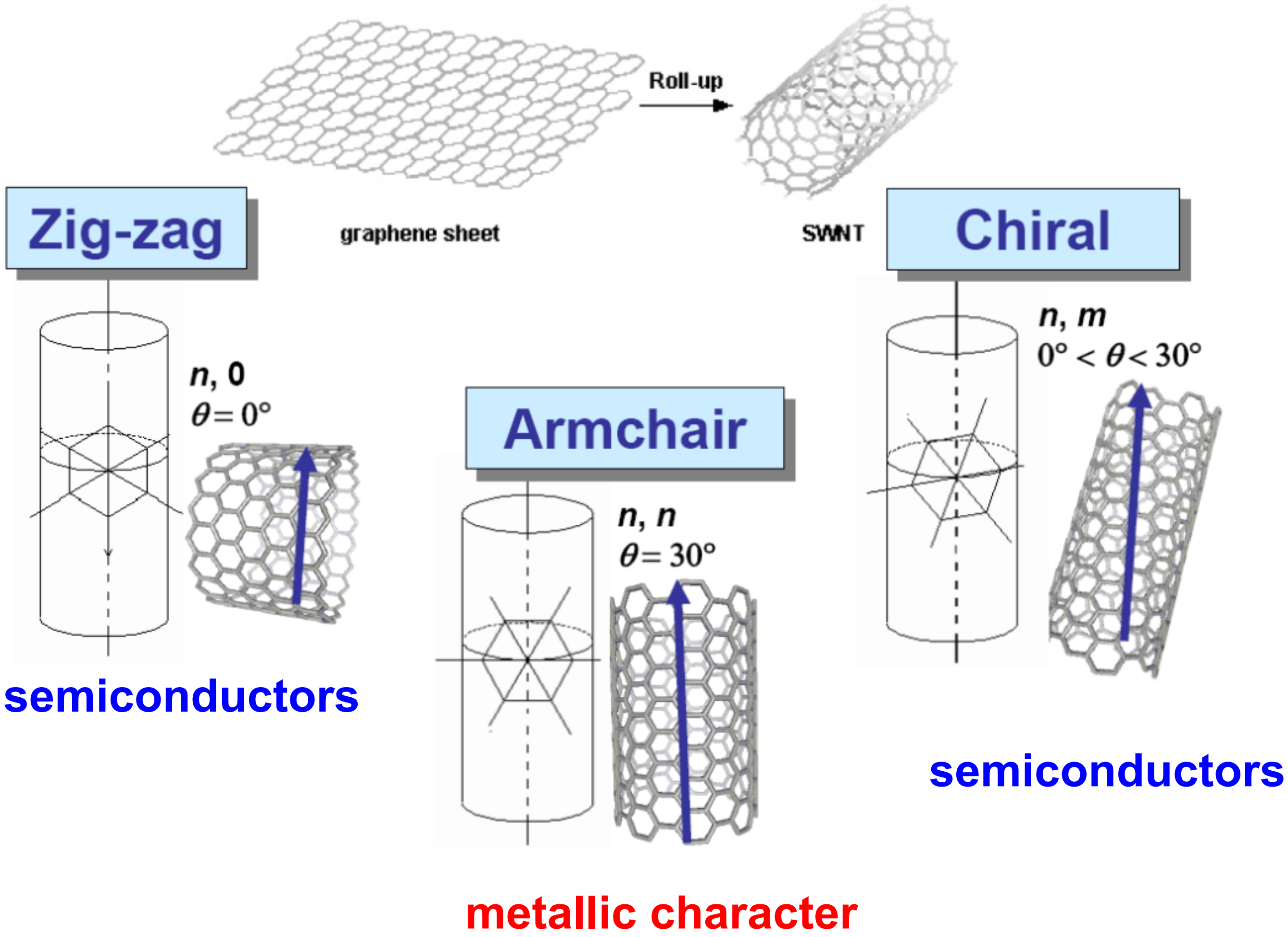
Roll-up
graphene sheet
SWNT
Zig-zag
n, 0
θ = 0°
semiconductors
Armchair
n, n
θ = 30°
metallic character
Chiral
n, m
0° < θ < 30°
semiconductors

Structure

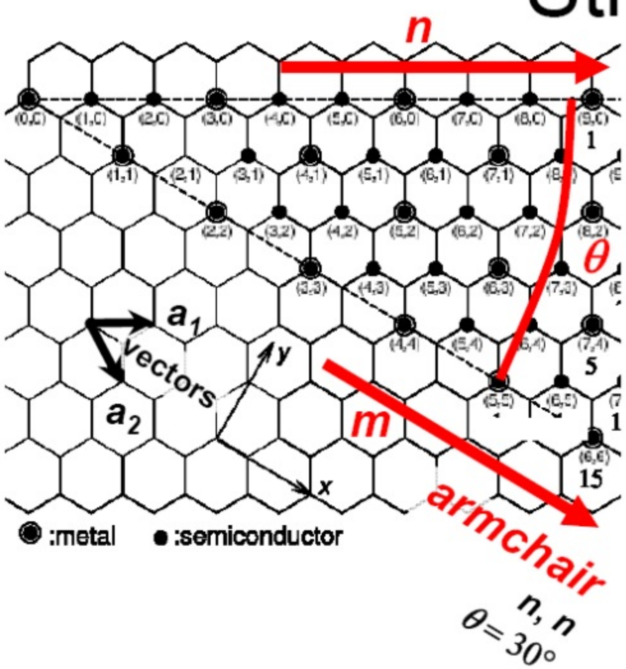

roll-up vector

$$C_h = n\hat{\mathbf{a}}_1 + m\hat{\mathbf{a}}_2$$

wrapping angle

$$\theta = \tan^{-1}[\sqrt{3}n/(2m+n)]$$

nanotube (*n*,*m*)

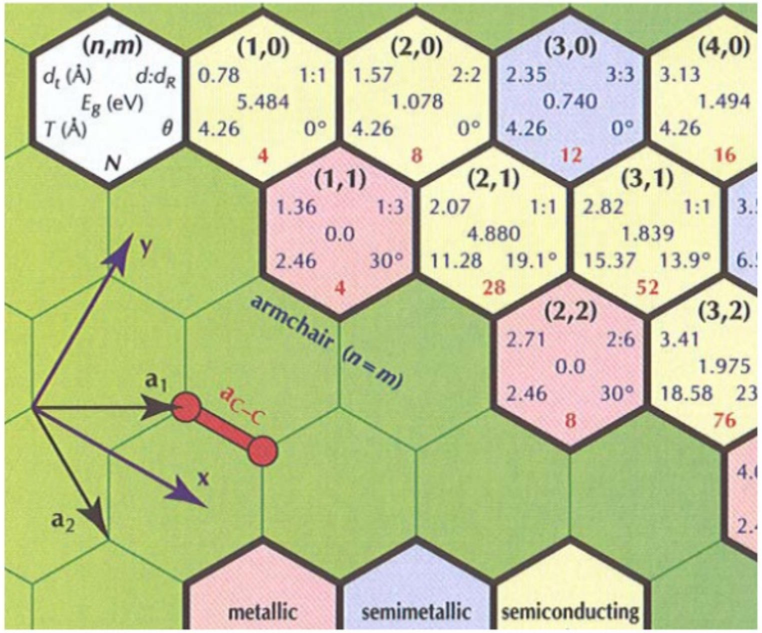

armchair SWCNT posses a **metallic character**
the other behave as **semiconductors**

CNTs structures

The integers *n* and *m* denote the number of unit vectors along two directions in the honeycomb crystal lattice of graphene.
If *m*=0, the nanotubes are called "zigzag".
If *n*=*m*, the nanotubes are called "armchair".
Otherwise, they are called "chiral".

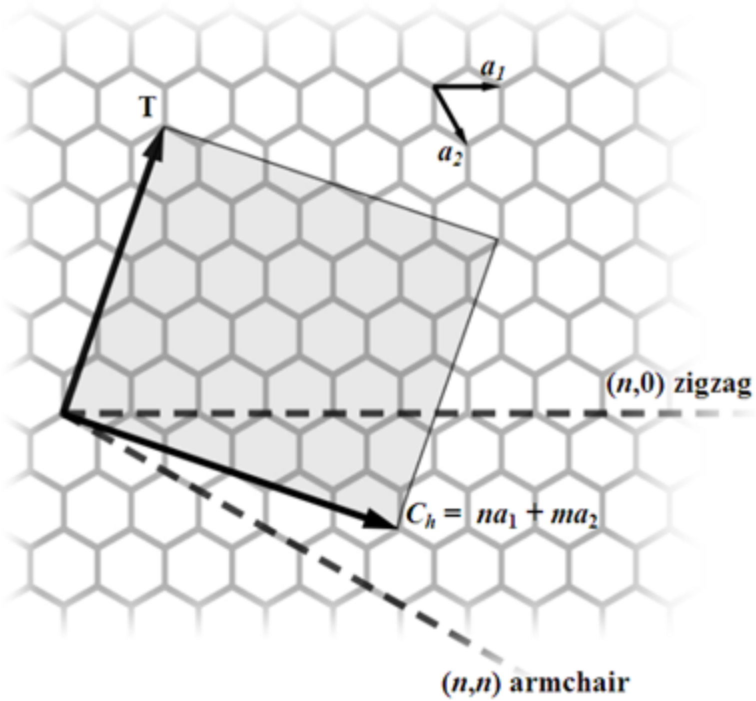

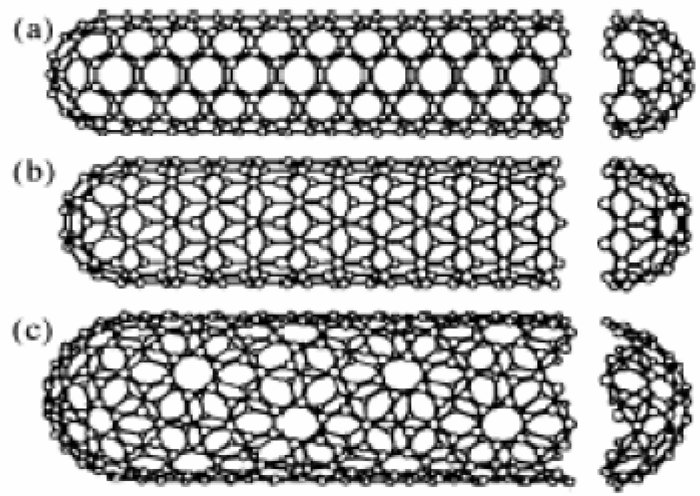

Some SWNTs with different chiralities. The difference in structure is easily shown at the open end of the tubes. a) armchair structure b) zigzag structure c) chiral structure

CNTs properties

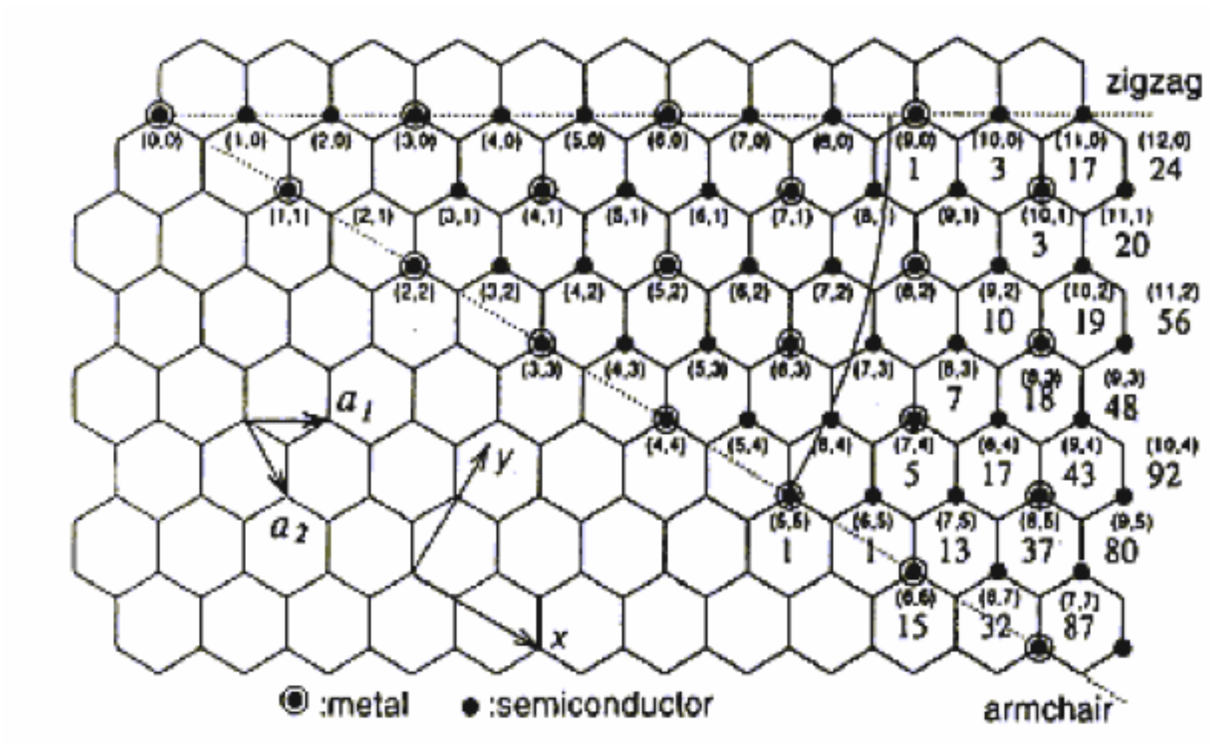

Figure 1-3: All possible structures of SWNTs can be formed from chiral vectors lying in the range given by this figure. (n,m) with n,m integer and m<=n or θ <30º.[5]

CNTs structures

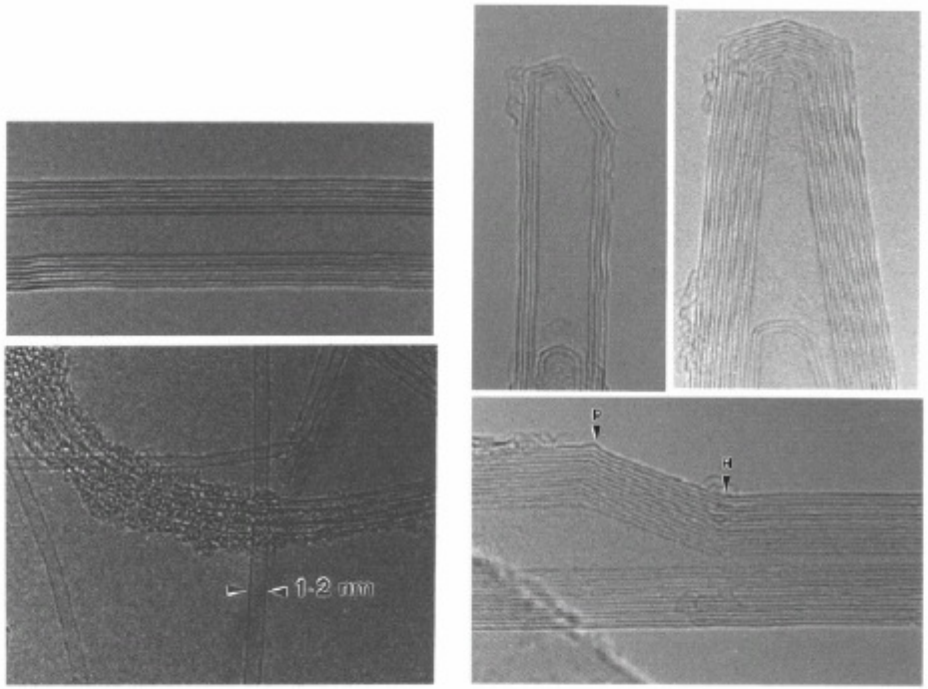

Figure 1-4: Different structures of MWNTs. Top-left: cross-section of a MWNT the different walls are obvious, they are separated by 0.34nm. Rotation around the symmetry axis gives us the MWNT. Top-right: Symmetrical or non-symmetrical cone shaped end caps of MWNTs. Bottom-left: A SWNT with a diameter of 1,2nm and a bundle of SWNTs covered with amorphous carbon. Bottom-right: A MWNT with defects. In point P a pentagon defect and in point H a heptagon defect.[6]

CNTs structures

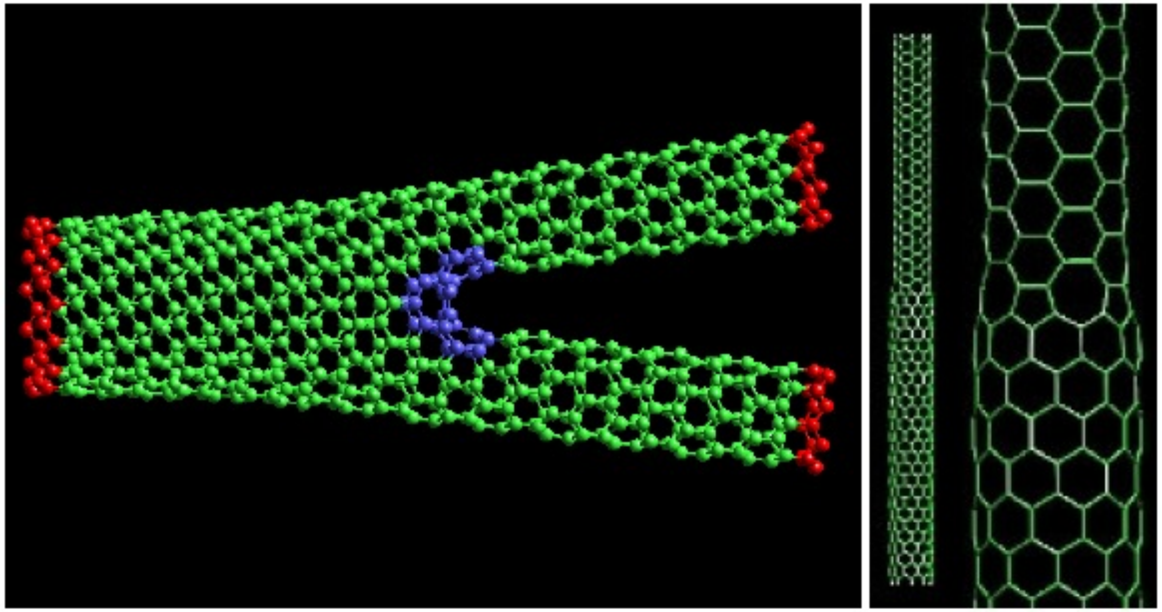

Figure 1-5: Left: A Y-branch, the defects are marked in blue. Right: A transition from a metallic to a semi-conducting SWNT. The change is made by insertion of pentagons and heptagons.

CNTs properties

SWNTs with different chiral vectors have dissimilar properties such as optical activity, mechanical, strength and electrical conductivity.

CNTs are 100 times stronger than steel

Comparison of Mechanical Properties

Material	Young's Modulus(1) (GPa)	Tensile Strength (GPa)	Elongation at Break (%)
SWNT	~1 (from 1 to 5)	13-53^E	16
Armchair SWNT	0.94^T	126.2^T	23.1
Zigzag SWNT	0.94^T	94.5^T	15.6-17.5
Chiral SWNT	0.92		
MWNT	0.8-0.9^E	150	
Stainless Steel	~0.2	~0.65-1	15-50
Kevlar	~0.15	~3.5	~2
Kevlar^T	0.25	29.6	

1. misura della durezza di un materiale elastico

(The tangent modulus of the initial, linear portion of a stress-strain curve is called *Young's modulus)*

Kevlar

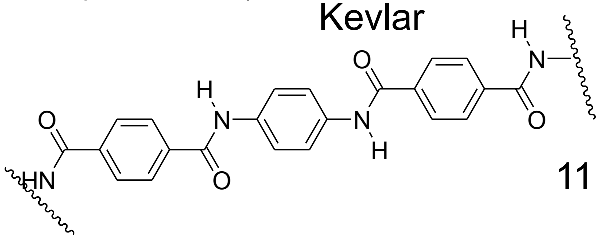

around $1500 per gram as of 2000

~$50–100 per gram as of 2007

Potential applications of CNTs

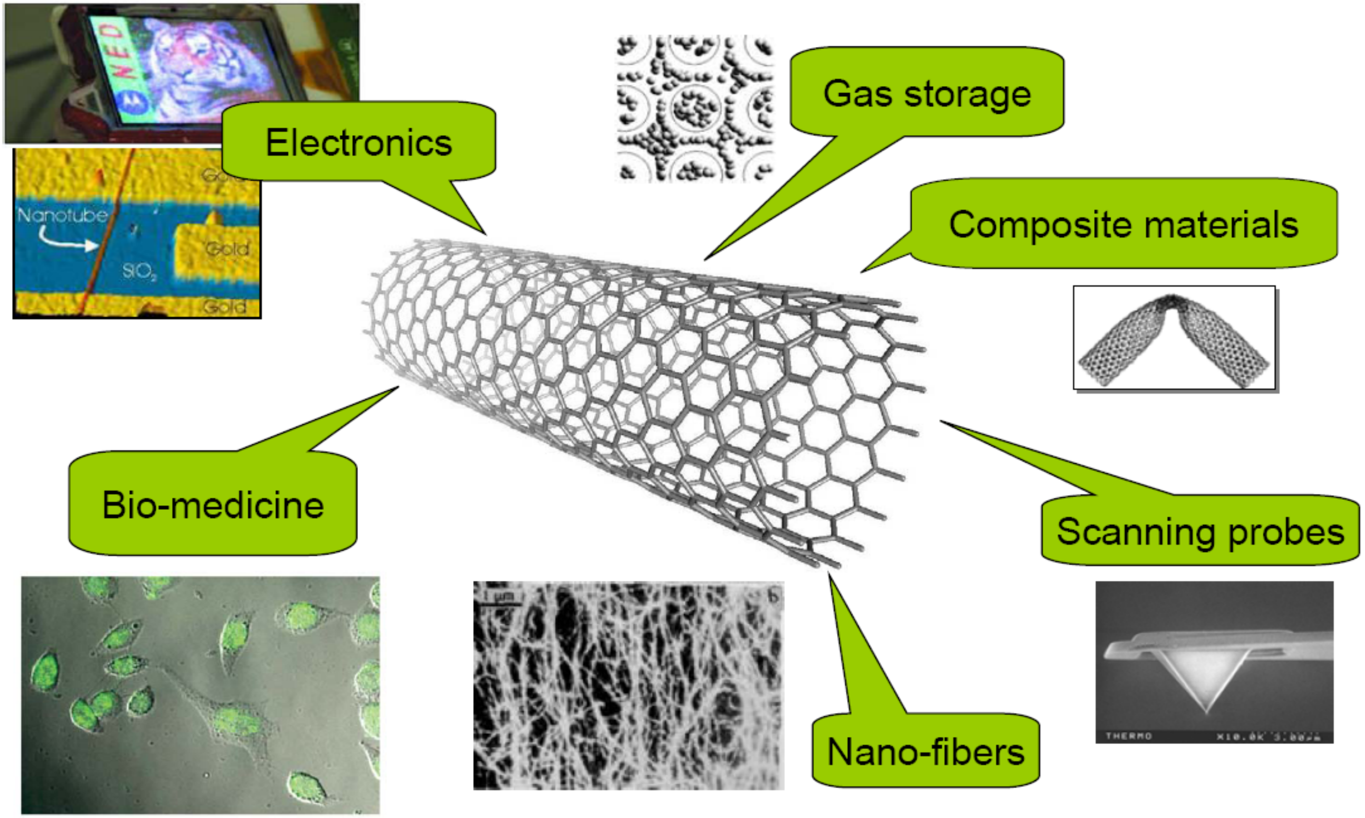

Synthesis: arc discharge

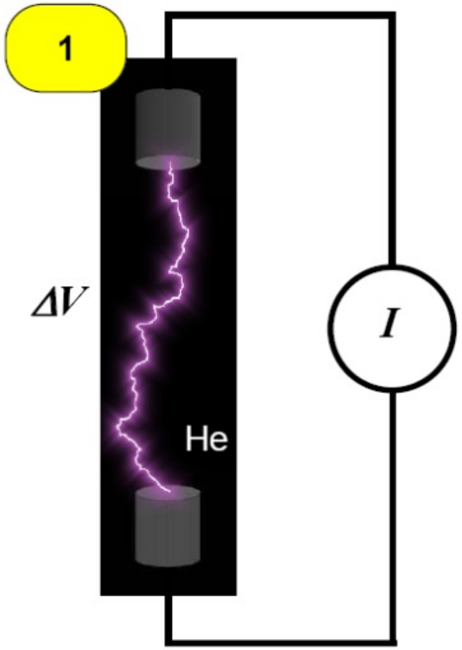

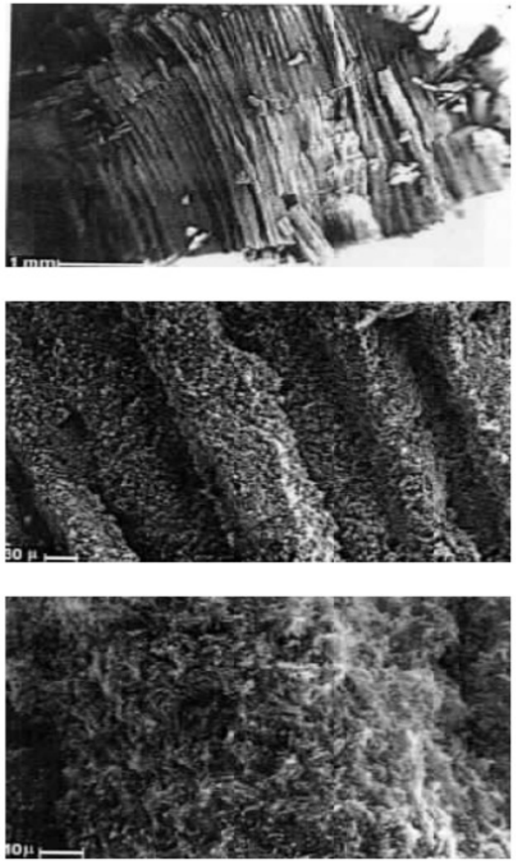

T = 3000 – 4000 °C (graphite mp)

Laser Ablation

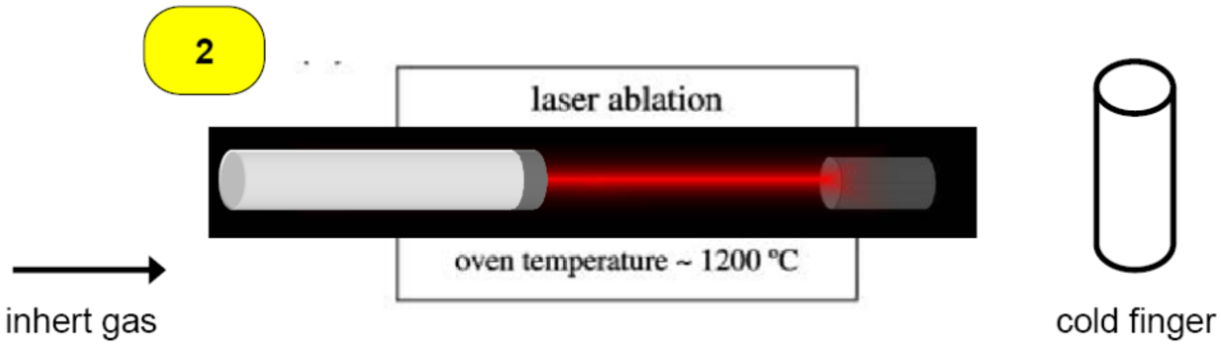

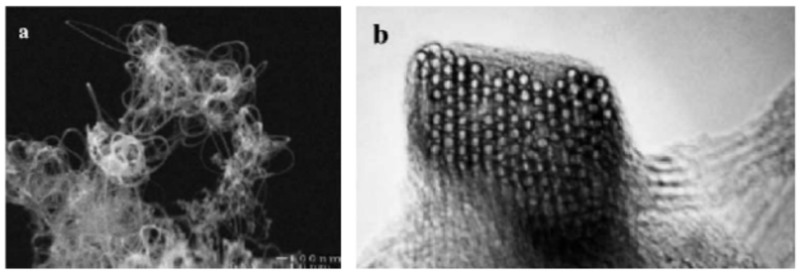

purification

Oxidation
- acid solution
- air at high T

Separation
- surfactants
- chromatography

Annealing

10.5 %

1 %

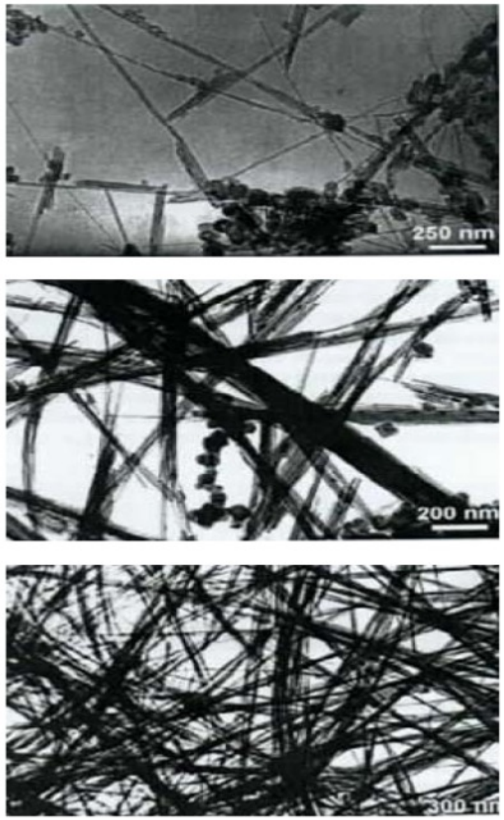

C. Furtado et al., *J. Am. Chem. Soc.* **2004**, *126*, 6095-6105

R. C. Haddon et al., *Mrs Bulletin* **2004**, *29*, 252-259.

Covalent Functionalization of CNTs

SCHEME 2. Oxidation of Carbon Nanotubes

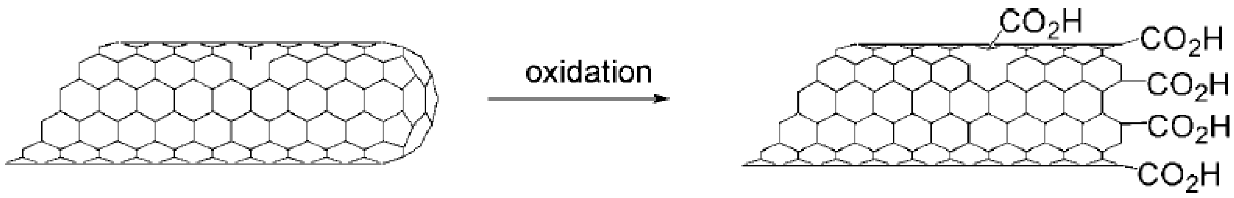

SCHEME 3. Amidation Reaction of Oxidized Carbon Nanotubes

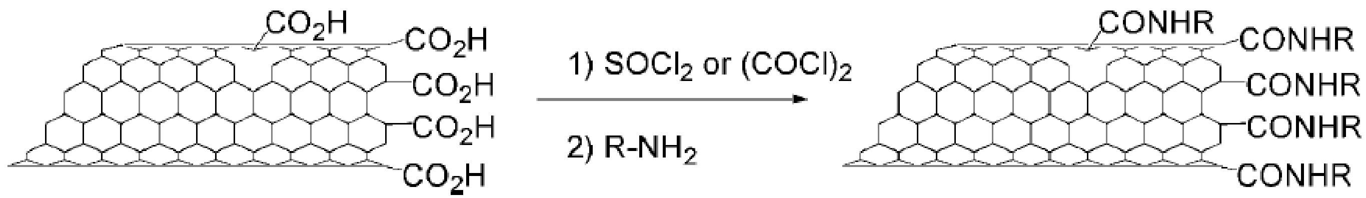

SCHEME 4. Functionalization of Carbon Nanotubes Using Addition Reactions (X = Functional Groups)

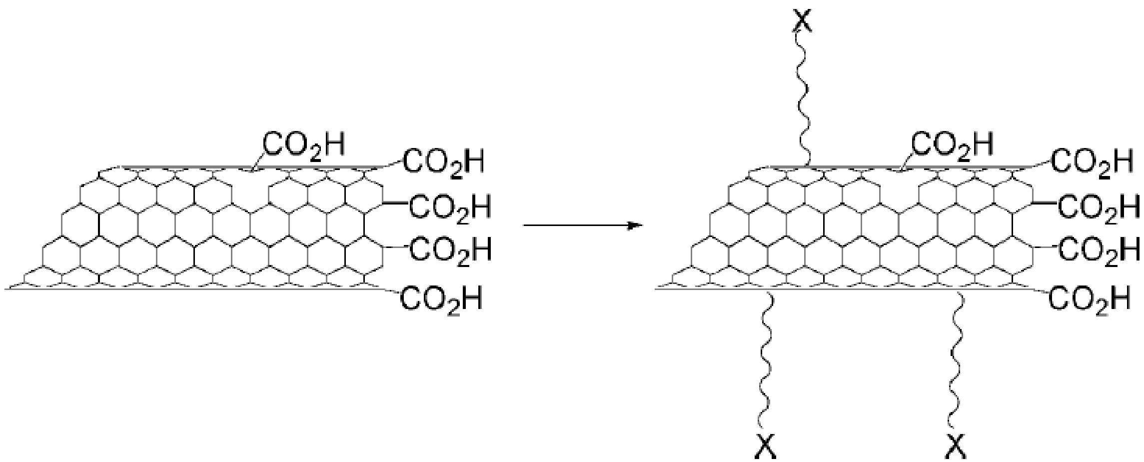

Carbon Nanotubes in Drug Design and Discovery *Prato et al.* **ACCOUNTS OF CHEMICAL RESEARCH** 2008, 41, 60-68.

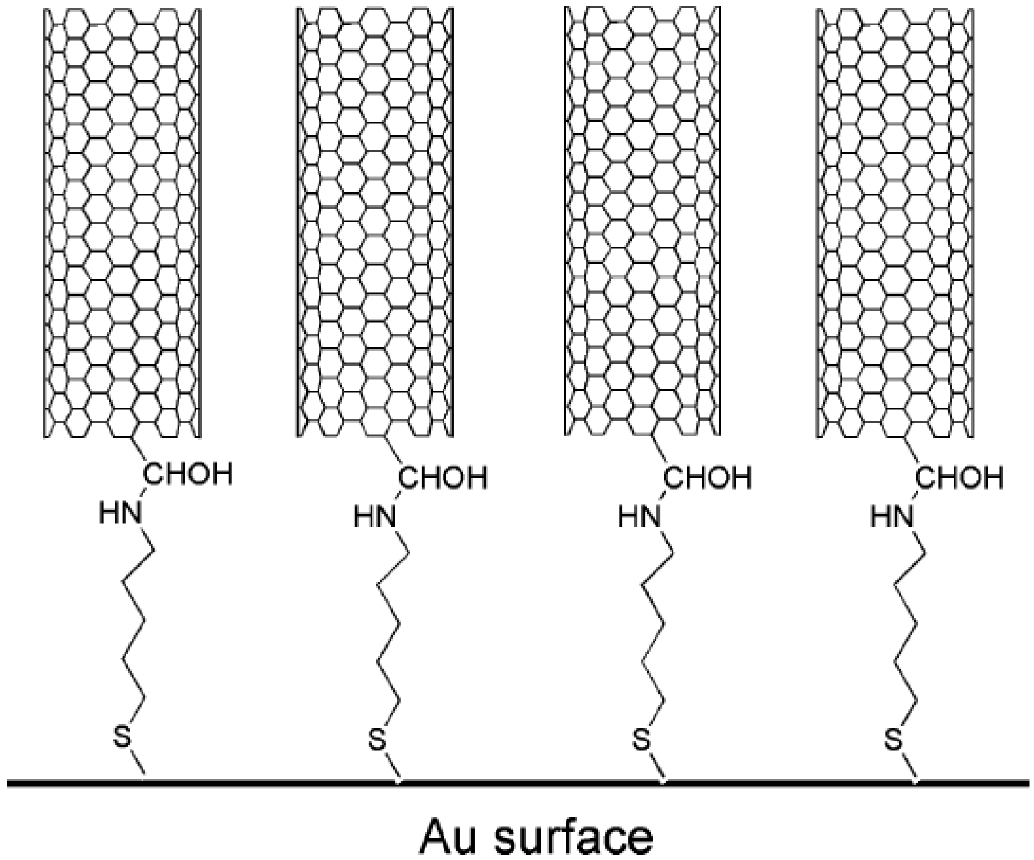

Figure 18. Controlled deposition of oxidized nanotubes onto gold surfaces by using aminothiols as chemical tethers.

D. Tasis, N. Tagmatarchis, A. Bianco, M. Prato Chem. Rev. **2006,** 106, 1105-1136

SCHEME 5. Insertion inside Carbon Nanotubes

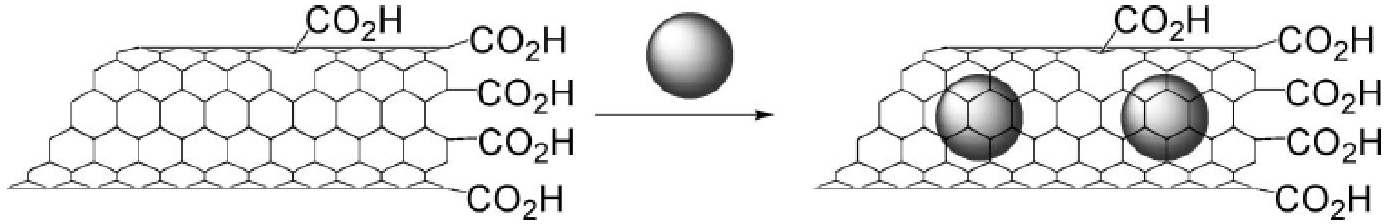

fullerenes, porphyrins, and metals, have indeed been included in the internal space of CNT, mostly due to hydrophobic interactions

TABLE 1. Molecular Structures of the Carbon Nanotube Conjugated with Different Therapeutic Agents

	Compounds	Bioassays
	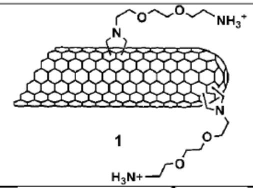 1	Cell internalization[24, 26, 27] Intracellular trafficking[24, 27] Cell viability[26] Plasmid DNA delivery[26, 32]
	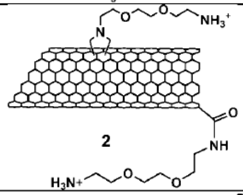 2	Precursor for the preparation of CNT **4** and **5**
fluorescein	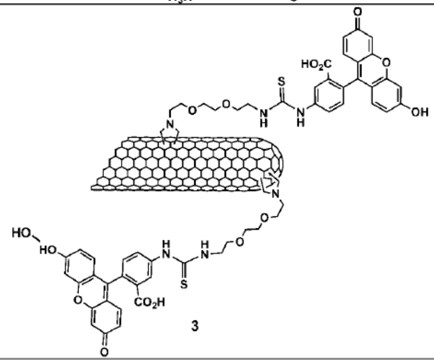 3	Cell internalization[23-25] Intracellular trafficking[23-25] Cell viability[23-25]
fluorescein	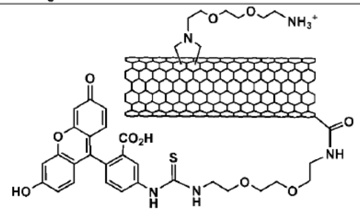 4	Cell internalization[24]
amphotericin B and fluorescein	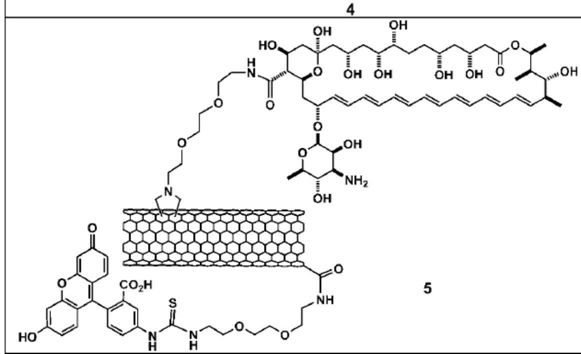 5	Cell internalization[22, 24] Cell viability[22]

TABLE 1. Continued

	Compounds	Bioassays
	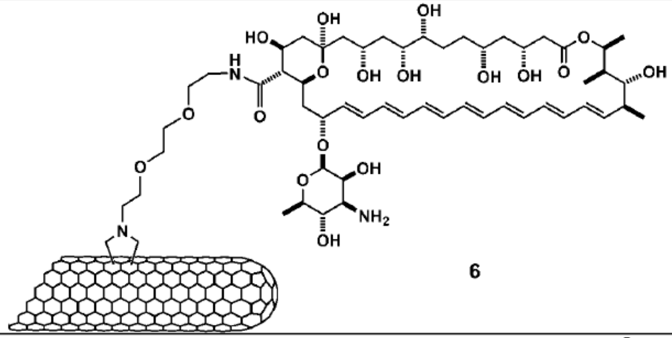 6	Antibiotic delivery[22]
anticancer agent methotrexate	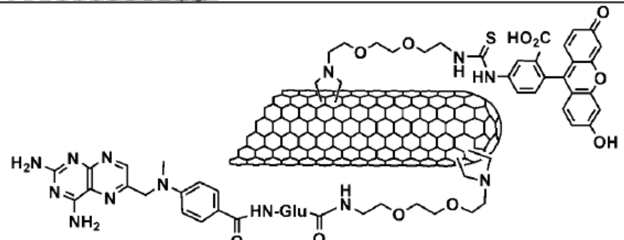 7	Cell internalization[36] Cell viability[36] Anticancer delivery[36]
immunogenic peptides	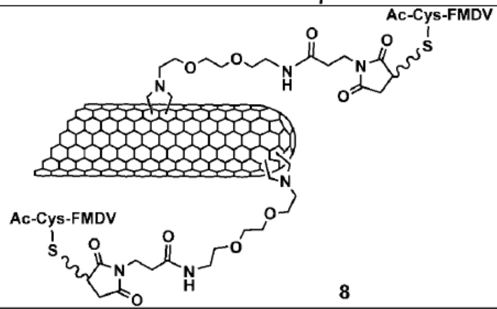 8	Immunogenic activity[41, 42] (FMDV peptide corresponds to the 141-159 region of the viral envelope protein VP1 from foot-and-mouth disease virus)
immunogenic peptides	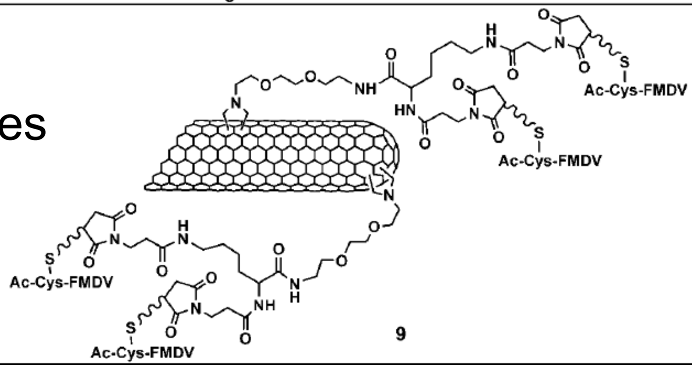 9	Immunogenic activity[42] (FMDV peptide corresponds to the 141-159 region of the viral envelope protein VP1 from foot-and-mouth disease virus)

Noncovalent Functionalization of CNTs

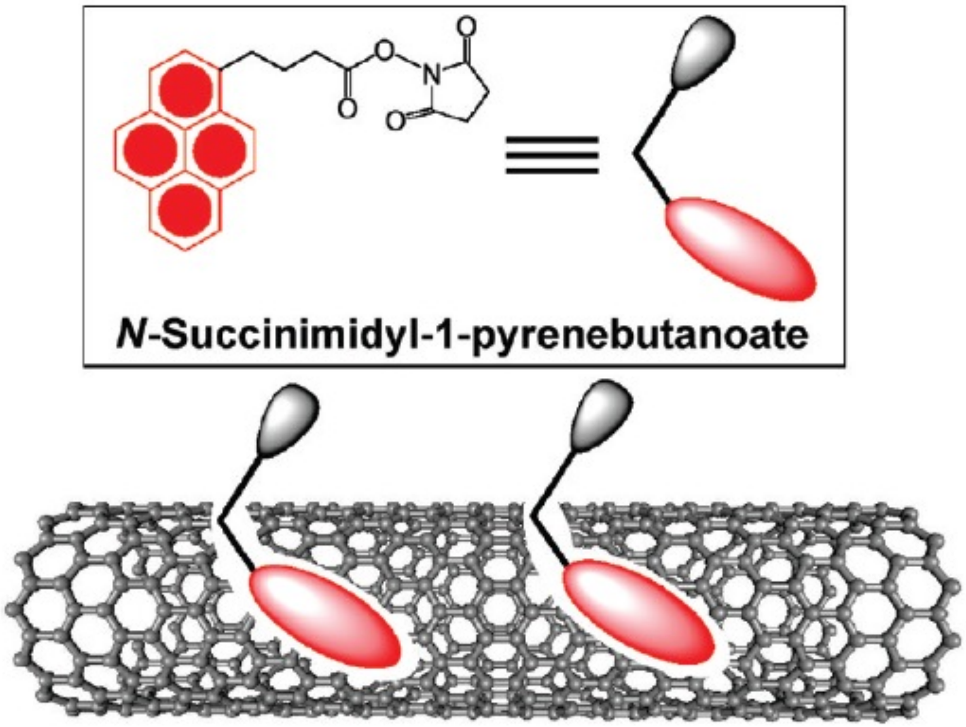

FIGURE 2. Schematic representation of *N*-succinimidyl-1-pyrenebutanoate-decorated SWNT.

Noncovalent Functionalization of SWNTs *Zhao and Stoddart* **ACCOUNTS OF CHEMICAL RESEARCH, 2009, 42,** 1161-1171.

modulation of the electrical conductance

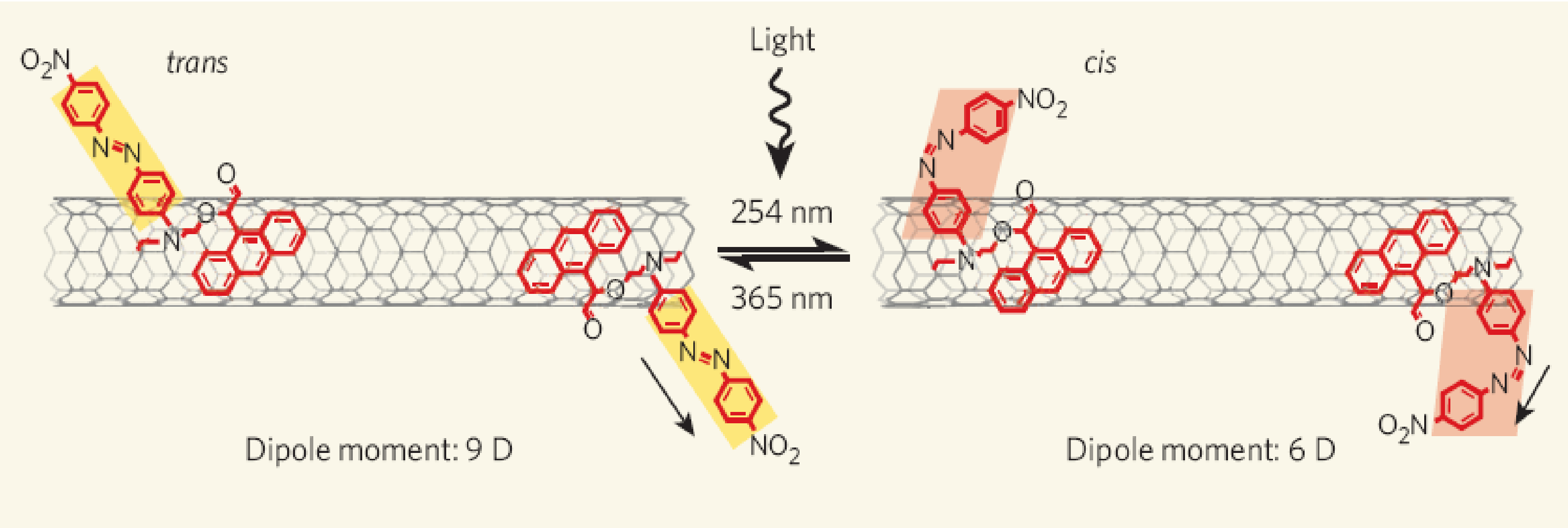

Figure 1 | Light bending and stretching. Simmons *et al.*[1] make the conductivity of carbon nanotubes responsive to light by adding molecules of the azo-based Disperse Red 1 dye to the nanotube walls. These dye molecules undergo photoisomerization, with their molecular conformation shifting around their central nitrogen double bond: from the *trans* to the *cis* form under ultraviolet light of wavelength 254 nm, and back again under blue light of 365 nm. The changes cause significant, reversible shifts in the molecules' electrical dipole moments (unit: debye, D; arrows indicate direction), and thus in the electrical conductance of a nanotube transistor as a whole.

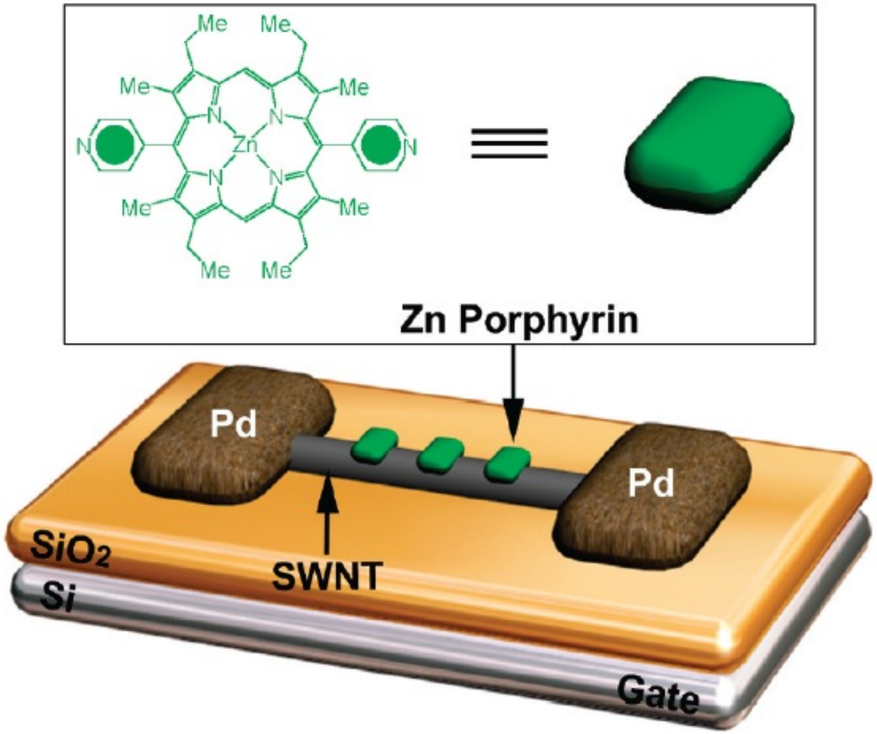

FIGURE 3. Schematic representation of the zinc porphyrin-coated SWNT/FET device employed for transistor measurements.

to detect photoinduced electron transfer between ZnPorphyrin and CNT

The SWNTs act as the electron donors, and the porphyrin molecules act as the electron acceptors. The photoresponse of the zinc porphyrin-coated SWNT/FET was investigated by its illumination with a light-emitting diode (LED) centered at 420 nm,

Hecht, D. S.; Ramirez, R. J. A.; Briman, M.; Artukovic, E.; Chichak, K. S.; Stoddart, J. F.; Gru¨ ner, G. Bioinspired detection of light using a porphyrin-sensitized singlewall nanotube field effect transistor. *Nano Lett.* 2006, *6*, 2031–2036.

FET field effect transistor

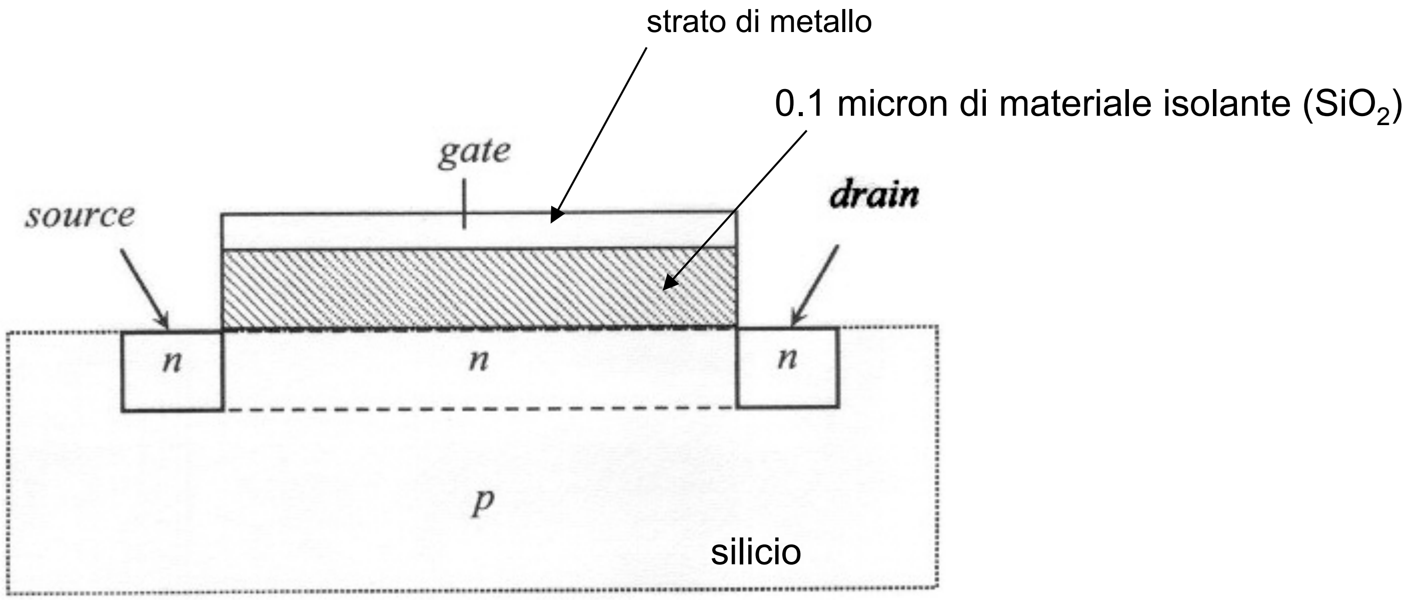

schema di un transistor ad effetto di campo

Quando si applica un voltaggio al *gate* si crea un campo che penetra nel semiconduttore e provoca, a seconda della polarità del voltaggio, un aumento o un decremento nel numero di elettroni che trasportano la corrente in questo canale. Quindi la corrente *source-drain* è modulata dal voltaggio del *gate*.

amplifica un segnale elettrico

sensori

serve as chemical sensors to detect nonfluorescent organic molecules selectively, on the basis of their molecular recognition by the cyclodextrin torus.

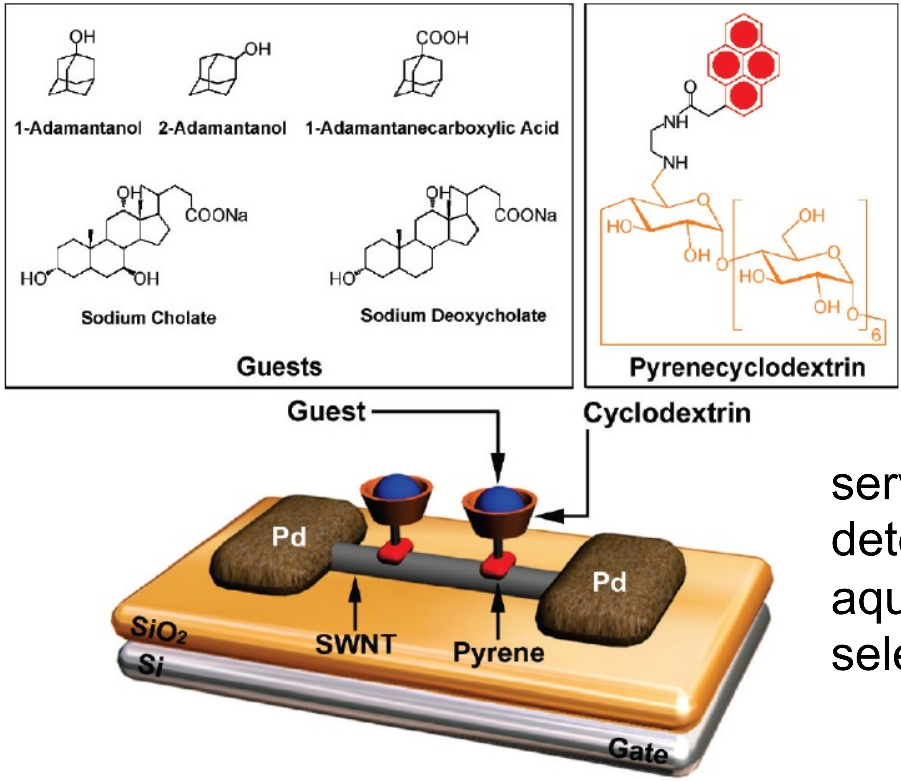

1-adamantanol > 2-adamantanol> 1-adamantanecarboxylic acid > sodium deoxycholate > sodium cholate.

serve as chemical sensors to detect organic molecules in aqueous solution, not only selectively but also quantitatively.

FIGURE 5. Schematic representation of the pyrenecyclodextrin-decorated SWNT/FET device showing how pyrenecyclodextrin-decorated SWNTs interact with guest molecules when they are being sensed in a FET device. The five guest molecules employed were 1-adamantanol, 2-adamantanol, 1-adamantanecarboxylic acid, sodium cholate, and sodium deoxycholate.

Satisfyingly, the magnitude of the transistor characteristic movements in the pyrenecyclodextrin-SWNT/FET devices in the presence of the organic molecules depends linearly upon the magnitudes of the complex formation constants (*K*S) exhibited by the pyrenecyclodextrin derivative with these molecules.

Zhao, Y.-L.; Hu, L.; Stoddart, J. F.; Gru¨ ner, G. Pyrenecyclodextrin-decorated singlewalled carbon nanotube field-effect transistors as chemical sensors. *Adv. Mater.* 2008, *20*, 1910–1915.

Hybrid CNTs-NPs materials

- Formation of metal nanoparticles directly on the carbon nanotube surface
- Connecting metal nanoparticles and CNTs

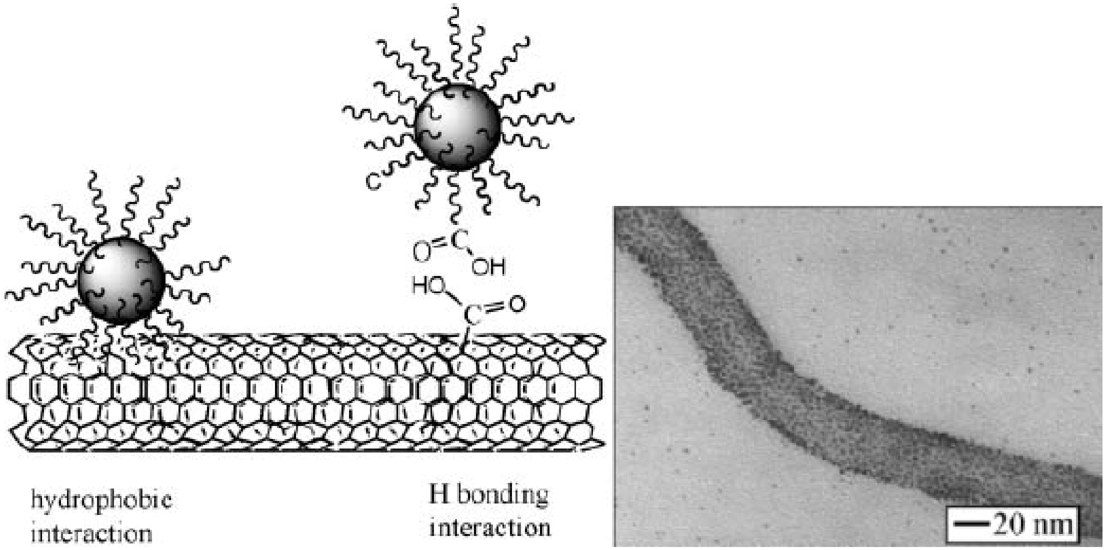

Fig. 14 Schematic illustrations of the assembly of mixed-monolayer capped NPs on oxidized CNTs and a characteristic TEM image of the resulting derivative (reproduced with permission from ref. 57).

"Decorating carbon nanotubes with metal or semiconductor nanoparticles".

V. Georgakilas, D. Gournis, V. Tzitzios, L. Pasquato, D. M. Guldi, M. Prato, *J. Mater. Chem.* **2007**, *17*, 2679-2694.

L. Han, W. Wu, F. L. Kirk, J. Luo, M. M. Maye, N. N. Kariuki, Y. Lin, C. Wang and C. J. Zhong, *Langmuir*, **2004**, *20*, 6019.

Connecting metal nanoparticles and CNTs

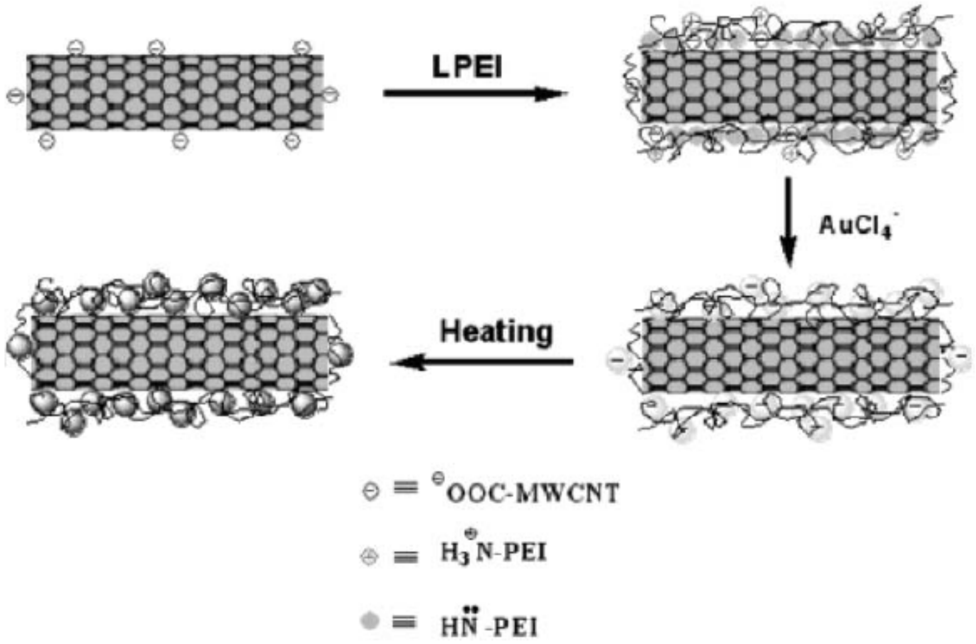

Fig. 22 Schematic illustration of the experimental procedure in which PEI possibly interacts with acid-functionalized MWNTs through electrostatic interaction and physisorption processes (reproduced with permission from ref. 73)

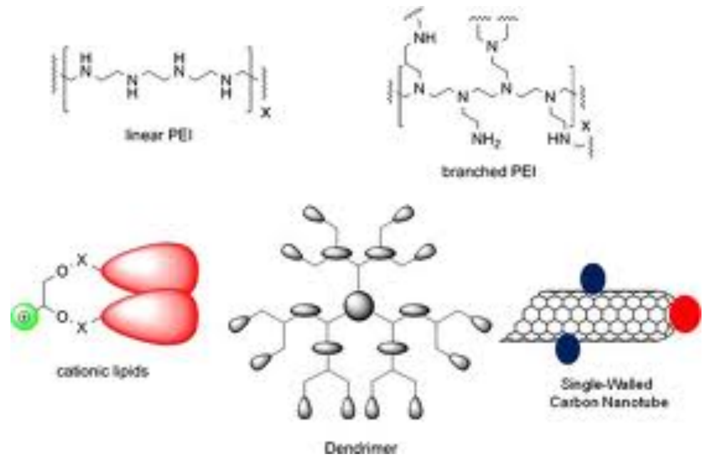

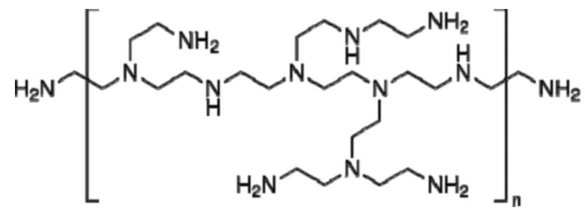

PEI = polyethyleneimine

X. Hu, T. Wang, X. Qu and S. Dong, J. Phys. Chem. B, 2006, 110, 853.

Aligning Au Nanorods by Using Carbon Nanotubes as Templates

Luis M. Liz-Marzan et al. *ACIE* **2005**, *44*, 2.

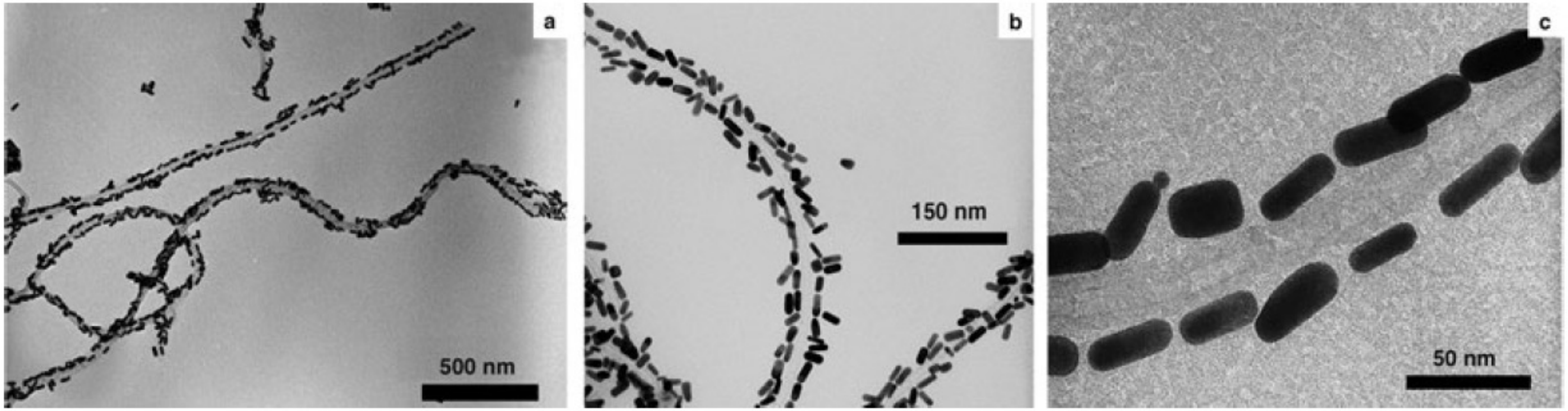

Figure 1. TEM images of Au nanorods (average aspect ratio 2.94), assembled on MWNTs (average diameter 30 nm) at various magnifications.

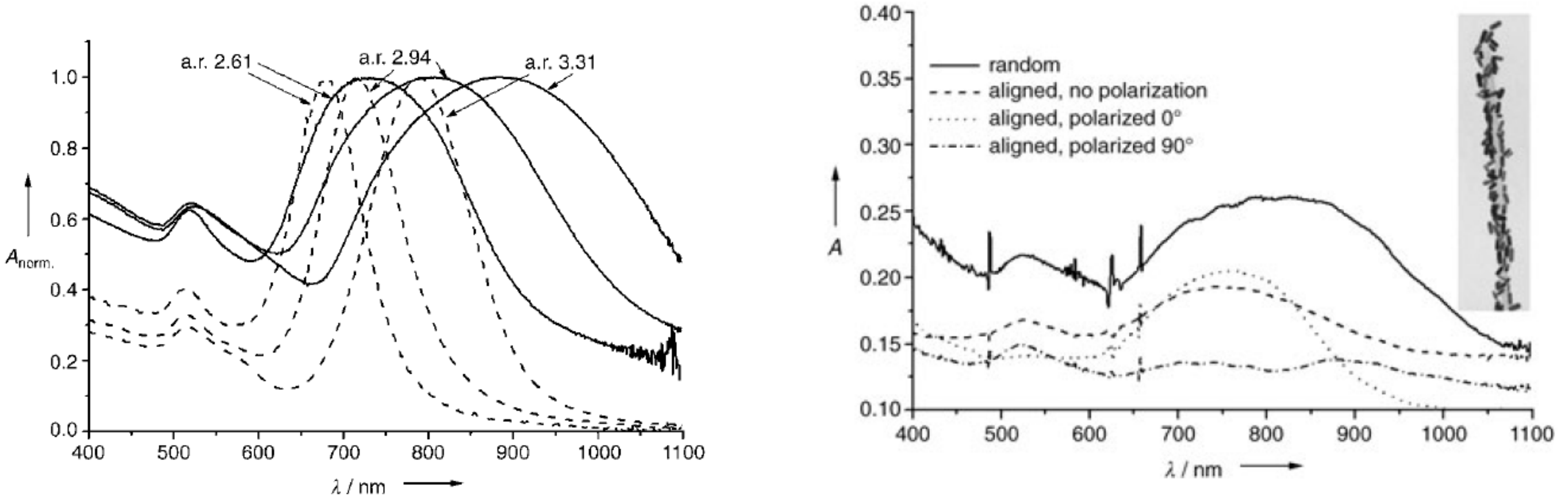

Figure 2. UV/Vis spectra of aqueous dispersions of individual Au nanorods (dashed lines) and nanorods attached on MWNTs (solid lines). The average aspect ratios (a.r.) of the nanorods are indicated.

Figure 3. UV/Vis spectra of Au nanorod/MWNT nanocomposites dispersed in a PVA film before (-----) and after (——) stretching. Spectra of the stretched film using polarized light (•••••: 0°; –•–•: 90°) are also shown. The aspect ratio of the rods is 2.94. The inset shows a TEM image of a stretched Au/CNT composite in PVA.

CNTs characterization

TEM, SEM, AFM

TGA

RAMAN spectroscopy (can distinguish between metallic and semiconducting CNT)

radial breathing mode Tangential modes

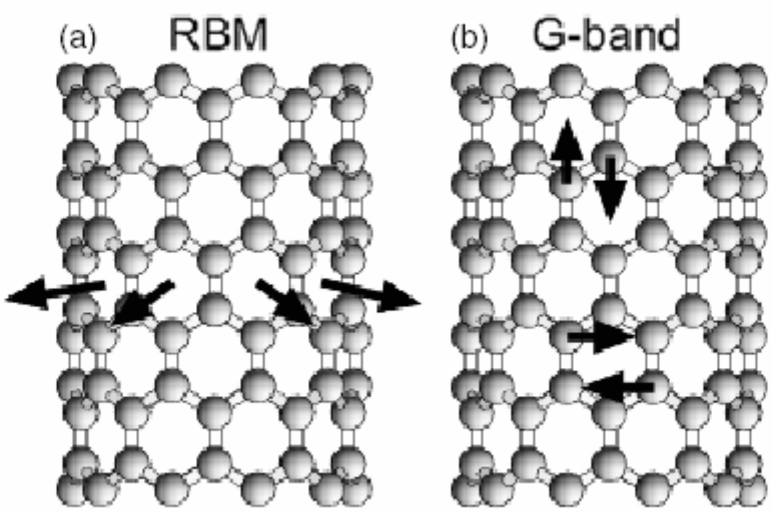

D-band

disorder-induced mode

120- 250 cm^{-1} multi-peak features at 1580 cm^{-1}

The frequency of the RBM can be used to determine the diameter of the nanotube.
RBM mode, in fact, is proportional to the inverse of the nanotube diameter.
For CNT with d < 2 nm the G band is used.

HiPCO SWCNT

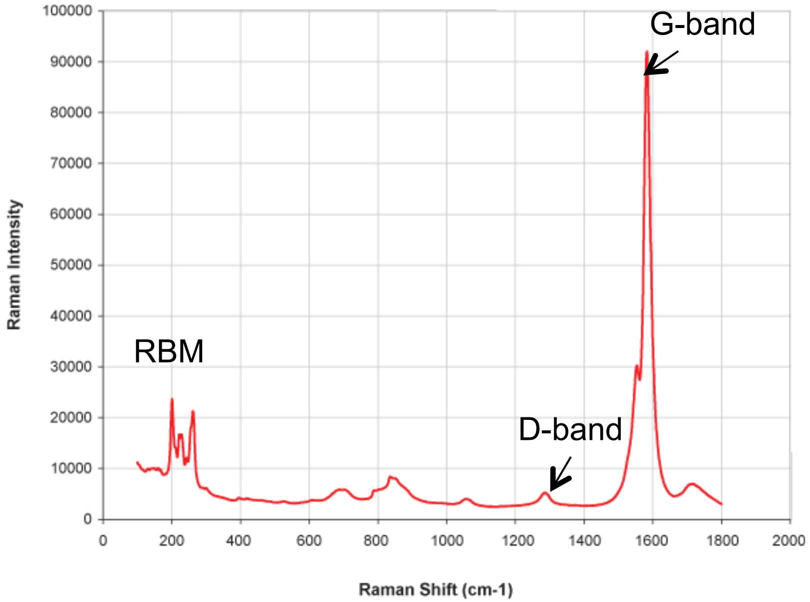

Raman spectrum of HiPCO SWCNTs using a laser wavelength of λexc = 633 nm.

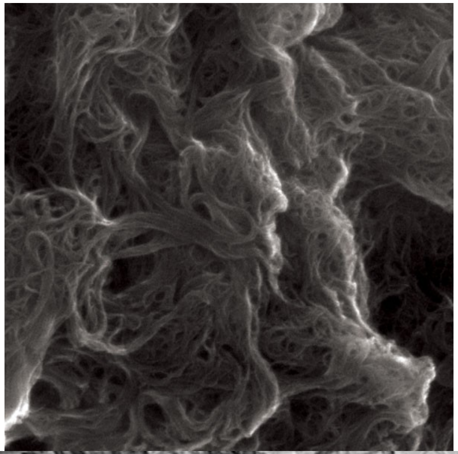

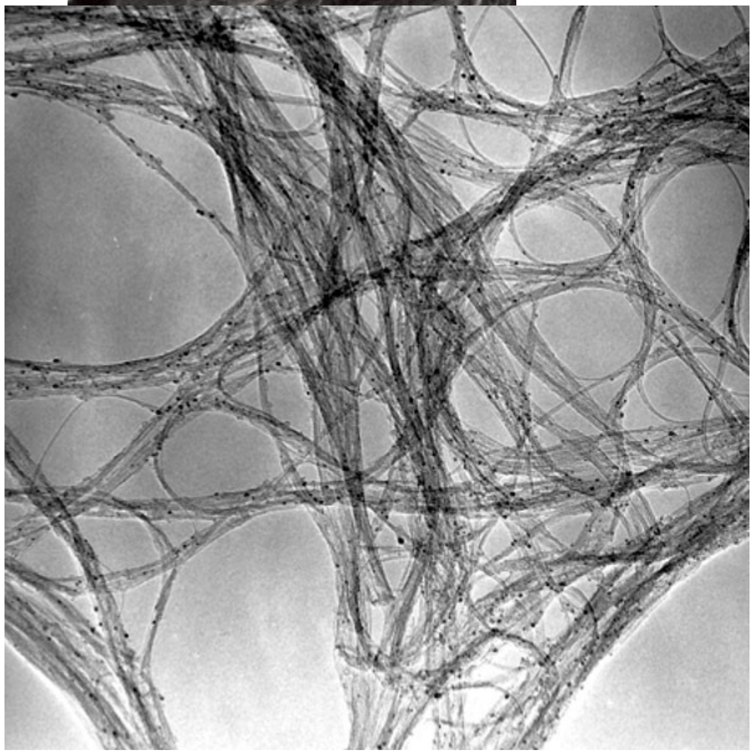

Single Wall Nano Horns

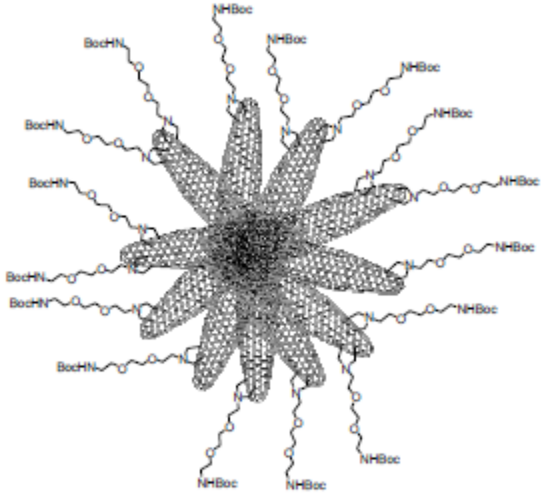

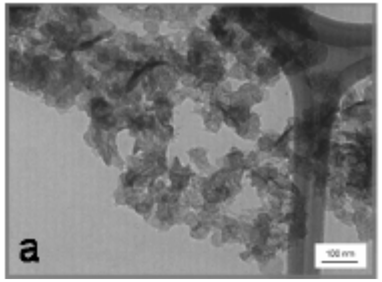

Carbon Nano Onions

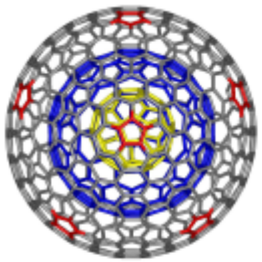

$C_{60}@C_{240}@C_{560}$

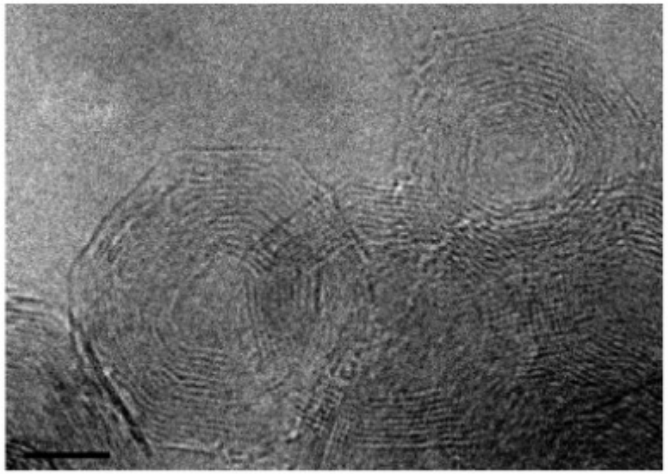

TEM picture of polyhedral CNOs.